Current Problems in Diagnostic Radiology 48 (2019) 172–183

Current Problems in Diagnostic Radiology

journal homepage: www.cpdrjournal.com

Pitfalls and Misinterpretations of Cardiac Findings on PET/CT Imaging: A Careful Look at the Heart in Oncology Patients

Sonia L. Betancourt Cuellar, MD[a,*], Diana Palacio, MD[b], Marcelo F. Benveniste, MD[a], Brett W. Carter, MD[a], Gregory Gladish, MD[a]

[a] Department of Diagnostic Radiology, The University of Texas MD Anderson Cancer Center, Houston, TX
[b] Department of Medical Imaging, The University of Arizona, Banner Medical Center, Tucson, AZ

A B S T R A C T

Positron emission tomography (PET) computed tomography (CT) with 2-[fluorine-18] fluoro-2-deoxy-D-glucose (FDG) has been established as an effective modality for evaluation of cancer. Interpretations of patterns of physiologic ^{18}F-FDG uptake by the heart is particularly difficult given the wide normal variations of ^{18}F-FDG metabolic activity observed. Atypical patterns of focal or diffuse physiologic cardiac ^{18}F-FDG uptake and post-therapeutic effects after radiation therapy, systemic diseases, or cardiomyopathy may also be confused with malignant disease on ^{18}F-FDG PET/CT. In this article, we review the variations of normal cardiac ^{18}F-FDG uptake observed in oncology patients and the appearances of other patterns of pathologic metabolic activity, related or not related to the malignancy being investigated, that may lead to false-negative and false-positive results.

Introduction

Currently 2-[fluorine-18] fluoro-2-deoxyglucose (^{18}F-FDG) positron emission tomography (PET) computed tomography (CT) is widely used in oncology patients for the purposes of initial disease staging, evaluation of response to therapy, and surveillance. This practice has led to the recognition of patterns of physiological ^{18}F-FDG uptake by different organs and systems, such as the brain, heart, kidneys, and gastrointestinal tract. Interpretation of this uptake in the heart is particularly challenging given the wide normal variations of ^{18}F-FDG metabolic activity observed. Given that the myocardium has one of the greatest metabolic demands of any organ, PET/CT studies are performed during fasting to decrease cardiac glucose metabolism, and thus ^{18}F-FDG PET/CT activity within the myocardium. Atypical patterns of focal or diffuse physiological cardiac ^{18}F-FDG uptake may lead to incorrect diagnosis of malignancy. Moreover, posttherapeutic effects after radiation therapy, systemic diseases, or cardiomyopathy may also be confused with malignant disease on ^{18}F-FDG PET/CT.

In this article, we review the metabolic activity in the heart during fasting and nonfasting stages as detected by ^{18}F-FDG PET/CT. The variations of normal cardiac ^{18}F-FDG uptake observed in oncology patients are discussed, as are the appearances of other patterns of pathologic metabolic activity, related or not related to the malignancy being investigated, that may lead to false-negative and false-positive results.

Normal Fasting Heart Metabolism and ^{18}F-FDG Uptake

Several sources are used to supply the high energy demands of the heart, including fatty acids, carbohydrates, and ketone bodies.[1] The metabolism of glucose by the heart depends on the available substrate and myocardial function and perfusion. After a meal, when plasma glucose and insulin levels rise, so do levels of the glucose transporters in the heart (GLUT-1 and GLUT-4), increasing the cardiac glucose uptake. Conversely, in the fasting state, plasma insulin levels decrease and most of the cardiac energy is supplied by fatty acids following reduction of the oxidative glucose metabolism obtained from carbohydrates.[2]

^{18}F-FDG PET/CT imaging in oncology patients is performed under a minimum of 4 hours of fasting, with the intent of capturing the images under fatty acid metabolism conditions, so that the normal background cardiac ^{18}F-FDG uptake is decreased to a minimum and may be easily differentiated from pathologic uptake. Even under strict and prolonged fasting conditions, the normal cardiac ^{18}F-FDG uptake varies widely in patients without intrinsic heart disease. Moreover, among patients undergoing multiple PET/CT studies, physiological uptake may vary in the same patient from study to study.[3] This variability may be explained by changes in the patient's metabolic status and hormonal variations at any point in time.[4]

* Reprint requests: Sonia L. Betancourt Cuellar, MD, Department of Diagnostic Radiology, The University of Texas MD Anderson Cancer Center, 1515 Holcombe Blvd., Houston, TX 77030
E-mail address: slbetancourt@mdanderson.org (S.L. Betancourt Cuellar).

https://doi.org/10.1067/j.cpradiol.2018.02.002
0363-0188/

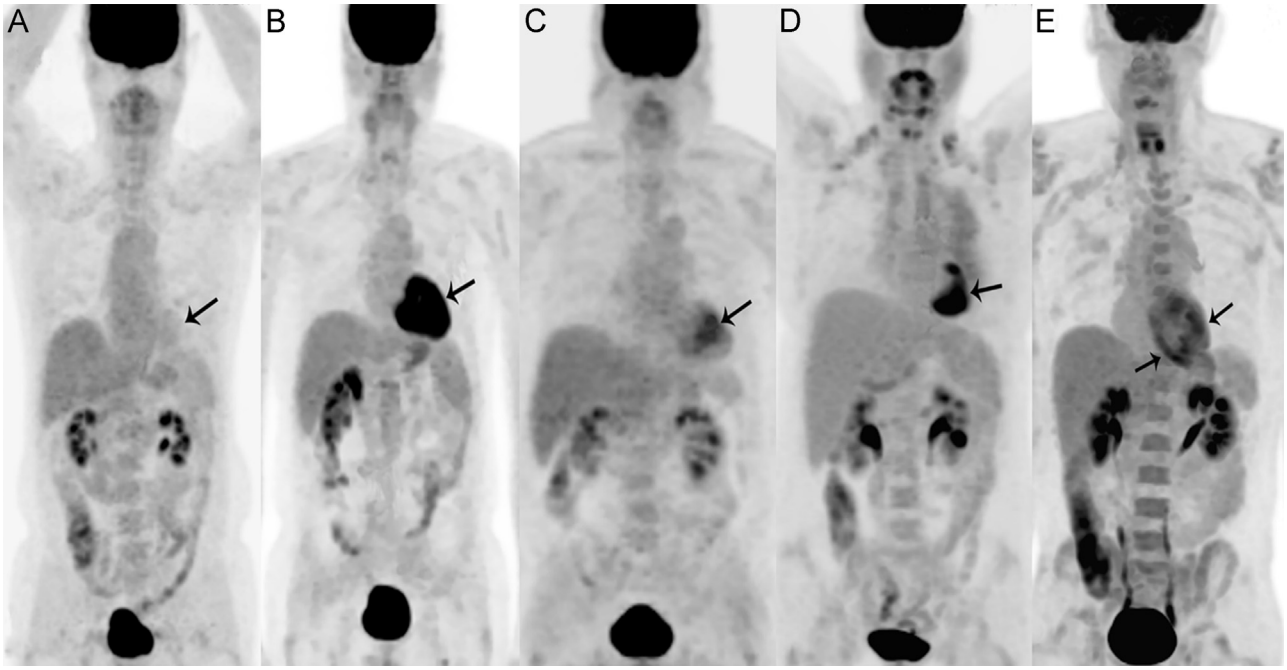

FIG 1. Normal variations of myocardial activity as seen on PET/CT imaging. (A, B, C, D, and E) maximum projection PET. (A) Absent myocardial activity. (B) Diffuse left ventricular uptake. (C) Basal ring uptake. (D) Lateral wall uptake. (E) Posterior wall uptake.

Physiological ^{18}F-FDG Uptake by the Heart

Myocardial Uptake Variability

After fasting for 4-6 hours, the physiological ^{18}F-FDG metabolic activity of the myocardium may be absent or may take the form of focal, regional, or diffuse uptake.[5-7] These patterns of ^{18}F-FDG uptake are not persistent or completely reproducible during repeated fasting, even for the same patient, and are not associated with parameters such as patient age, glucose level, weight, or dose of FDG uptake. Notably, Inglese et al[4] suggested that myocardial metabolism and ^{18}F-FDG uptake are influenced by systemic variables such as serum concentrations of metabolites and related hormones and also by unknown variables that are specific to each myocardial cell and to each time point. These patterns are related to qualitative distribution of ^{18}F-FDG within the myocardium without specific clinical significance.

Left Ventricular Uptake

A variety of physiological patterns of ^{18}F-FDG uptake may be seen in the left ventricle on FDG PET/CT imaging (Figs 1 and 2). Absent or faint ^{18}F-FDG uptake is indicative of either no uptake by the myocardium or low uptake compared to the mediastinum. A focal ^{18}F-FDG uptake pattern within the left ventricular papillary muscles is most frequently seen in combination with some activity of the adjacent myocardium, but in rare instances, papillary muscle ^{18}F-FDG uptake may occur in isolation. This may be potentially confused with thrombus or neoplasm, especially when it involves the posterior muscle, which sometimes demonstrates a globular shape.[8] Regional ^{18}F-FDG activity is usually significantly lower in the septum and anterior left ventricular wall than in the lateral and posterior walls.[3,4,9,10] Regional uptake at the base of the heart and posterolateral region is a recognized physiological pattern and apparently is more common in patients who have previously undergone radiation therapy to a field near the heart.[4,5] A "ring pattern" of ^{18}F-FDG uptake represents diffuse accumulation in the basal wall. Variations of this patterns include "over half ring pattern" and "spot pattern," characterized by focal accumulation of ^{18}F-FDG within diffuse uptake. The diffuse pattern consists of homogeneous and diffuse uptake in the left ventricular wall.[4,5]

Atrial Uptake

Given the minimal amount of energy spent by the atria compared to the ventricles, atrial ^{18}F-FDG uptake is uncommon in physiological conditions but it can be occasionally seen as faint FDG-uptake[11] (Fig 3). Increased atrial FDG activity with or without chamber

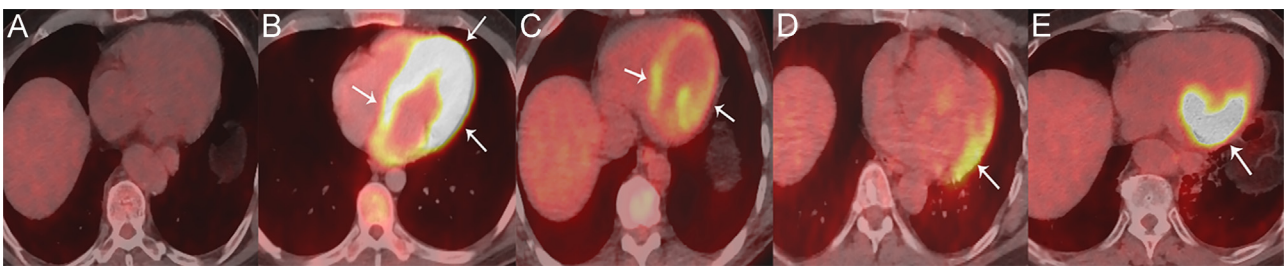

FIG 2. Normal variations of myocardial activity as seen on PET/CT imaging (A, B, C, D, and E) fused axial PET/CT demonstrating normal patterns of physiological left ventricular FDG uptake. (A) Absent myocardial activity. (B) Diffuse left ventricular uptake. (C) Basal ring uptake. (D) Lateral wall uptake. (E) Posterior wall uptake. (Color version of figure is available online.)

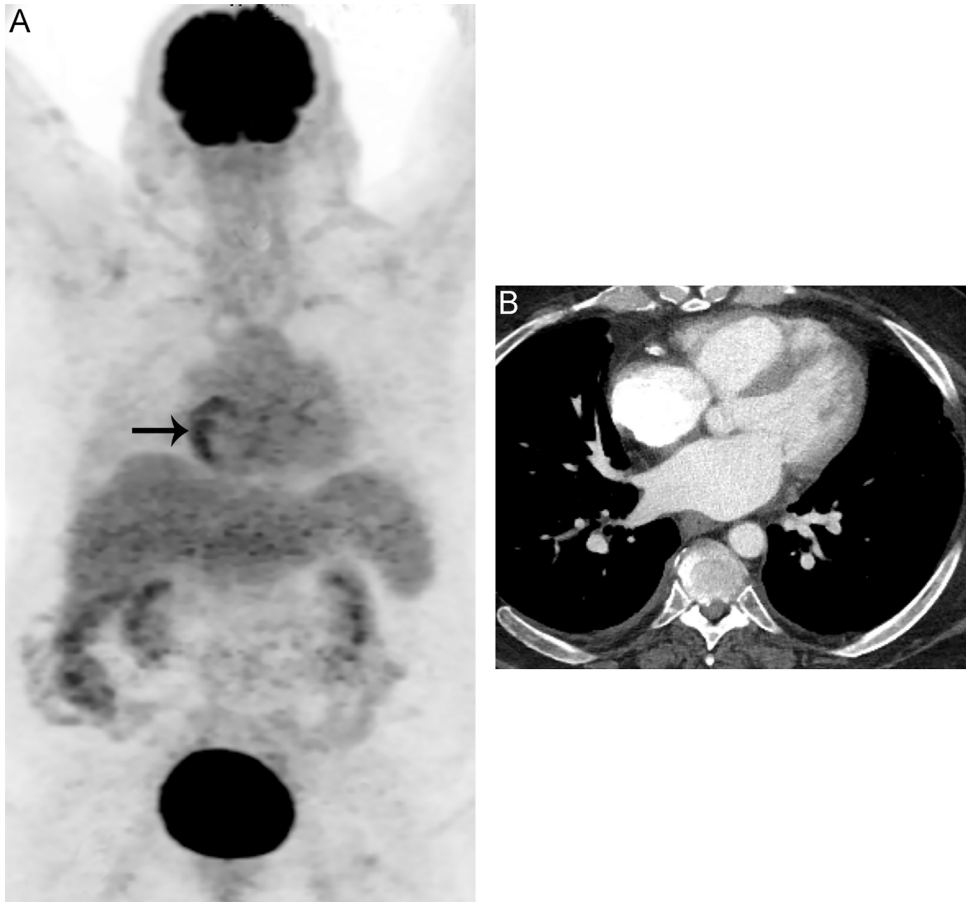

FIG 3. Subtle FDG uptake within the right atrium in a woman with multiple myeloma. (A) Maximum intensity projection PET image shows focal FDG uptake along the right heart border (black arrow). (B) Axial contrast-enhanced CT image shows no anatomical abnormality and normal appearance of the right atrium.

enlargement is rare and usually associated with cardiac disease, specifically atrial fibrillation.[12] The right atrial wall and the right atrial appendage are rare sites of ^{18}F-FDG uptake (Fig 4) and could potentially be confused with mediastinal adenopathy or with malignant pericardial infiltration, particularly if some degree of misregistration occurs.[13,14]

Crista Terminalis

The crista terminalis is a smooth, vertically oriented ridge that separates the right atrium from the right atrial appendage.[15] This structure originates from regression of the septum spurium as the sinus venosus is incorporated into the right atrial wall. The regression of the crista terminalis shows substantial variation, and thus the thickness of the crista terminalis varies widely in adults, ranging usually from 3-6 mm.[16] Several case reports have documented a prominent crista terminalis on different imaging modalities mimicking a right atrial mass.[15,16] As this muscular band may show increased ^{18}F-FDG uptake, it may be confused with tumor, thrombus, or focal pericardial metastases (Fig 5). Characterization of intraluminal tumor or thrombus in the atrial appendages owing to low contractility and stasis in patients with a clinical history of atrial fibrillation, prosthetic mitral or tricuspid valve, or stenotic mitral or tricuspid valve may require identification of the corresponding mass-like lesion on the CT

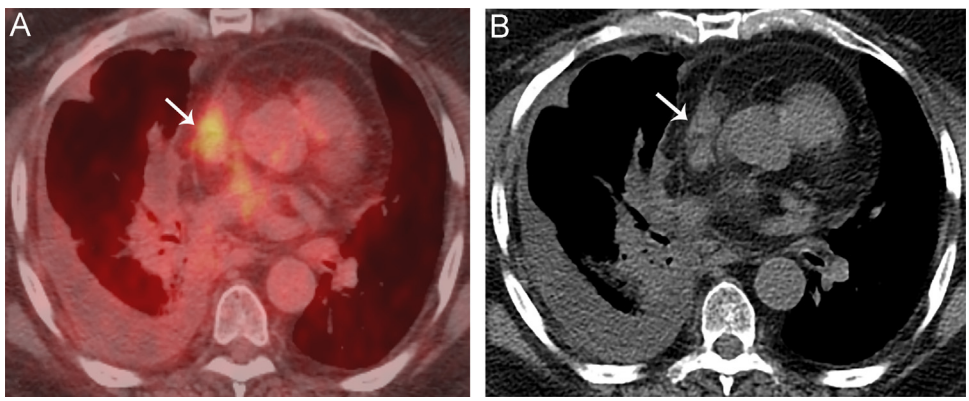

FIG 4. Increased metabolic activity in the right atrial appendage in a patient with a clinical history of clinical history of non–small cell lung carcinoma treated with radiation therapy 2 years ago. (A) Fused axial PET/CT shows diffuse FDG-uptake in the right atrial appendage. (B) Axial CT at the same level demonstrates no anatomical abnormality. (Color version of figure is available online.)

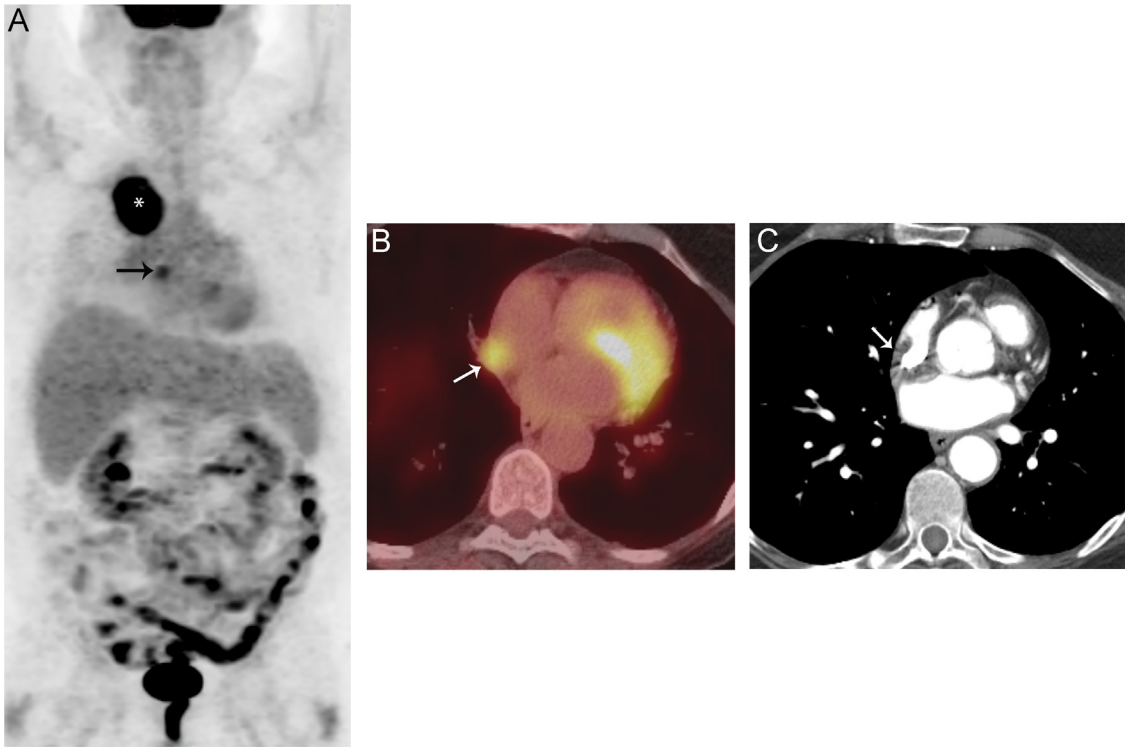

FIG 5. Increased FDG uptake at the crista terminalis in a woman with recurrent non–small cell lung carcinoma. (A) Maximum intensity projection FDG PET image shows focal FDG uptake in the heart (black arrow). The recurrent tumor (*) in the right upper lobe is FDG avid. (B and C) Fused PET/CT (B) and axial CT (C) images localize the FDG uptake in the right atrium at the crista terminalis (white arrow). (Color version of figure is available online.)

images or other available cross-sectional imaging.[17,18] Interestingly, it has been noted in the case of atrial thrombi that patients with right atrial involvement often will have concurrent left atrial thrombi.[19]

Right Ventricular ^{18}F-FDG Uptake

Physiological linear ^{18}F-FDG uptake has occasionally been described in the right ventricle in patients without heart disease.[7] Increased and diffuse ^{18}F-FDG accumulation in the right ventricle has been identified in the setting of increased ventricular pressure or overload in patients with pulmonary hypertension. The ratio of left to right ventricular ^{18}F-FDG uptake may provide information about right ventricular function.[20] In patients undergoing pneumonectomy, increased ^{18}F-FDG uptake has also been associated with increased pulmonary pressures.[7,21]

Abnormal ^{18}F-FDG Uptake in Nonmalignant Conditions

Atrial Fibrillation

Atrial fibrillation is characterized by rapid and irregular atrial contractions. During atrial fibrillation, the increased frequency of atrial contraction increases atrial metabolic demand. Diffusely increased ^{18}F-FDG activity of the atria associated with atrial fibrillation has been reported (Fig 6). Fujii et al[12] reported increased metabolic activity in the right atrial wall in 8 of 11 patients with atrial fibrillation. The marked rise in atrial oxygen requirements as a result of increased atrial metabolic demands in atrial fibrillation has been postulated as the explanation for the increased atrial ^{18}F-FDG uptake.[22] In addition to atrial fibrillation, other conditions such as congestive heart failure, atrial septal defect, or myocarditis also may demonstrate diffuse ^{18}F-FDG uptake of the atrial walls.[23]

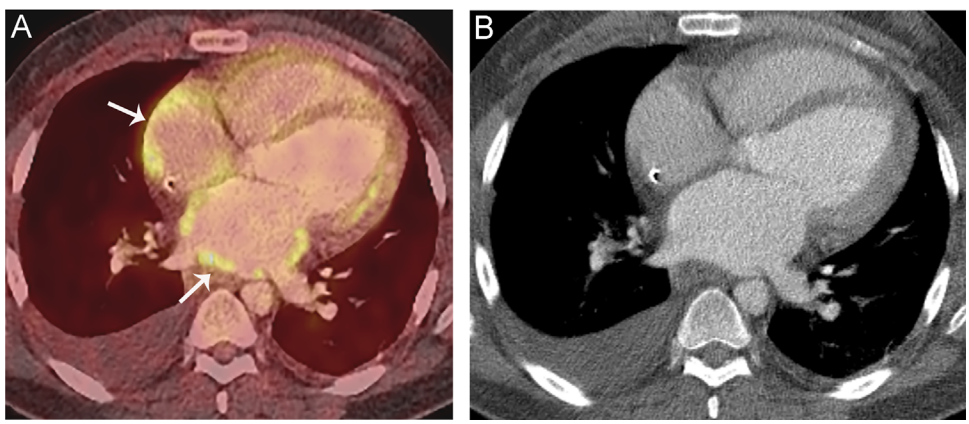

FIG 6. Increased FDG activity in the atria secondary to atrial fibrillation in a patient with a clinical history of lymphoma. (A) Fused axial PET/CT image shows increased FDG activity in the atria (arrows). (B) Axial contrast-enhanced CT image shows dilation of the atria. Right pleural effusion is present. (Color version of figure is available online.)

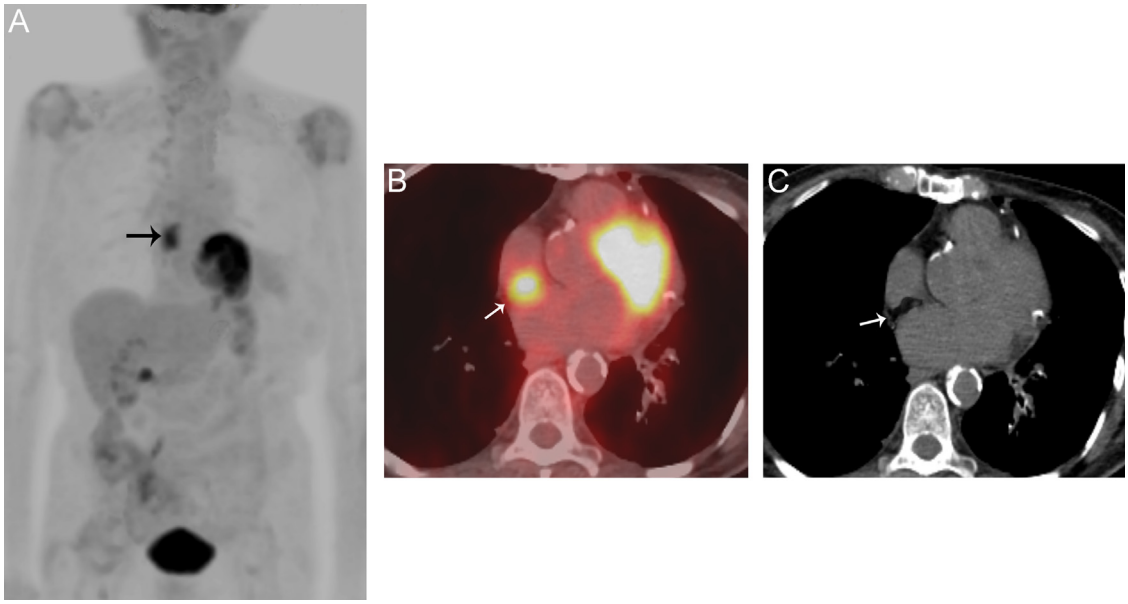

FIG 7. Brown fat activity within lipomatous hypertrophy of the interatrial septum in a man with treated non–small cell lung cancer. Maximum intensity projection FDG PET (A), fused axial PET/CT (B), and axial CT (C) images show focal FDG uptake in the right heart at the fat containing interatrial septum (arrows). (Color version of figure is available online.)

Lipomatous Hypertrophy of the Interatrial Septum

Lipomatous hypertrophy of the interatrial septum (LHIS) is an incidental finding associated with aging and obesity, with a prevalence of up to 8%.[24] LHIS is characterized by an increase of interatrial fat, which infiltrates the myocardial fibers.[25] An interatrial septal thickness >2 cm is considered diagnostic of LHIS.[26] In most patients this condition is asymptomatic, although LHIS has been associated with supraventricular arrhythmias, syncope, and sudden death.[25,27]

On cross-sectional imaging, LHIS has a mass-like bulging appearance located in the interatrial septum, usually extending to the atrial wall but rarely to the interventricular septum, and typically with sparing of the fossa ovalis.[28] Unlike intracardiac lipomas, the fatty lesions of LHIS are not encapsulated and histologically are composed of mature adipocytes and fetal fat cells or brown fat.[29] LHIS is confirmed by the presence of non-enhancing fat density on CT or fat signal intensity on MRI within a lesion arising in the atrial septum.

In a series that included 11 patients with LHIS examined with PET/CT, 9 (82%) of these patients showed focal increased FDG uptake corresponding to the region of LHIS on cross-sectional imaging. The reported mean standard uptake value (SUV) of the atrial septa was 5.6. Not all patients with LHIS in this series presented with increased FDG uptake, a finding the authors attributed to the presence of brown fat, which varies among patients with LHIS[30] (Fig 7). Brown fat also creates focal areas of ^{18}F-FDG uptake localized to the mediastinum around the pericardium and epicardium in up to 1%-2% of patients[31] (Fig 8).

Epipericardial Fat Necrosis

Pericardial fat necrosis is an uncommon benign condition of unknown etiology. Fat necrosis is common in the breast and has also been described affecting the subcutaneous fat, the peripancreatic fat in cases of pancreatitis, the epiploic appendages and, less frequently, the epipericardial fat.[32] Elevated intrathoracic pressure

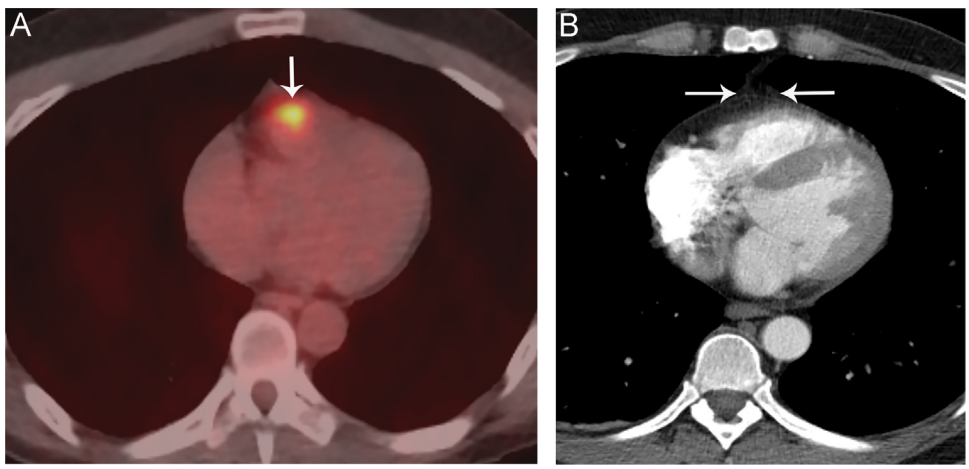

FIG 8. Brown fat activity in a man with a soft tissue sarcoma undergoing initial disease staging. (A) Fused PET/CT image demonstrates a focal area of FDG uptake in the anterior mediastinum that was initially considered suspicious for metastasis. (B) Corresponding axial CT image demonstrates only the presence of fat in the anterior mediastinum. (Color version of figure is available online.)

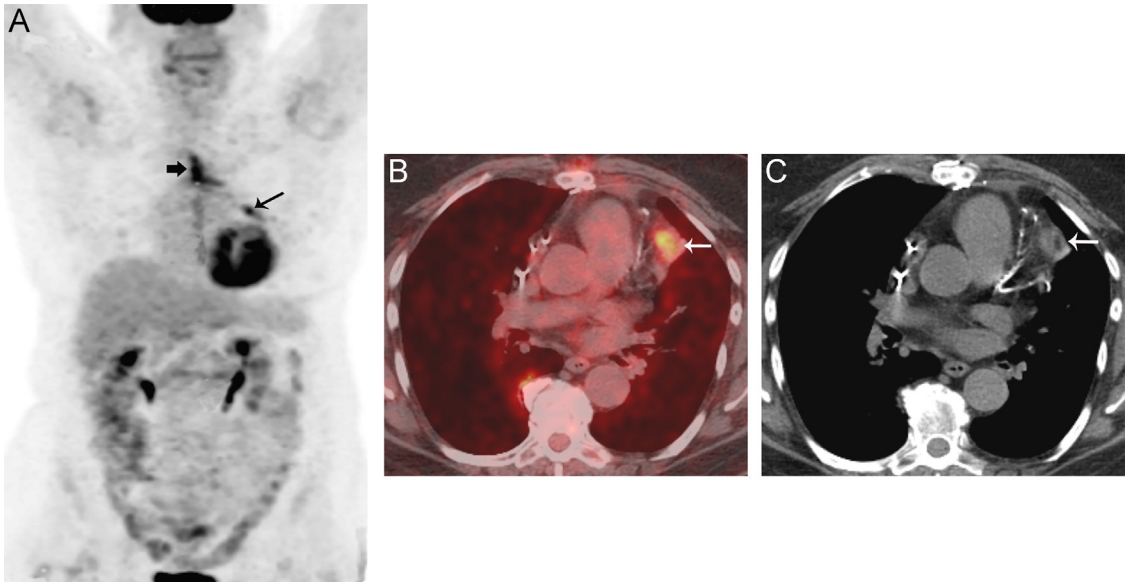

FIG 9. Fat necrosis in a woman with lymphoma undergoing restaging after a coronary artery bypass graft procedure. (A) Maximum intensity projection FDG PET image shows linear increased metabolic activity (short arrow) at the previous sternotomy. Focal FDG uptake is identified in the left mediastinum (long arrow). (B and C) Fused PET/CT (B) and axial CT (C) images demonstrate FDG uptake and increased density within the fat along the left anterior pericardium (white arrows), which is consistent with fat necrosis. (Color version of figure is available online.)

secondary to a Valsalva maneuver, acute torsion, or trauma has been proposed as the possible cause of pericardial fat necrosis.[32,33]

Clinically, this entity presents with sudden onset of low anterior chest pain on either the left or right side[34] that may vary with changes in the patient's position.[32] Epipericardial fat necrosis may demonstrate low-grade ^{18}F-FDG uptake on PET/CT images, representing the inflammatory nature of this process. On the axial CT component of FDG PET/CT, the presence of increased pericardial fat density, dense strands and thickening of the adjacent pericardium, and focal hypermetabolism on fusion ^{18}F-FDG PET/CT images at the affected area strongly suggest the diagnosis[32] (Fig 9).

Radiation-Induced Pericarditis

Radiation therapy is an essential part of multimodality therapy for malignancies such as breast cancer, lung cancer, lymphoma, and invasive thymomas, unfortunately it may induce pericardial disease and myocarditis. Recent modifications in radiation dose and delivery have reduced the incidence of cardiac complications, but the exact cardiac risks of contemporary regimens remain unknown.[35] The lower dose threshold for radiation associated with heart disease is around 15 Gy, with cardiac complication frequency increasing at doses greater than 40 Gy.[36] ^{18}F-FDG PET/CT examination should be delayed for 8-12 weeks after radiation therapy so that the expected ^{18}F-FDG-avid radiation effects, which can interfere with image interpretation, will be reduced.[37] In most cases, performing imaging 2-3 months after completion of radiation therapy seems clinically appropriate, as patients rarely develop clinical problems during the first 3 months after treatment.[38-40]

Radiation-associated pericarditis may be acute, developing during or immediately after radiation therapy, or delayed, typically presenting around 1 year after the end of radiation treatment. Both acute and chronic pericarditis usually manifest as an asymptomatic pericardial effusion. Radiation injury to the pericardium may also lead to fibrosis. Up to 20% of patients who experience late significant fibrosis of the pericardium after radiation therapy may initially have had an effusion.[41]

Correlation with the radiation ports is invaluable information, as it helps distinguish radiation-induced pericarditis from potential malignant pericardial involvement. Patients with radiation-induced pericarditis typically present with ^{18}F-FDG uptake confined to the radiation field.[5] The axial CT component of ^{18}F-FDG PET/CT images will demonstrate absence of focal nodularity or masses[5] (Fig 10).

The PET/CT SUV has been proposed as a way of differentiating malignant from benign pericardial ^{18}F-FDG uptake.[42,43] In a study of 34 patients with pericardial effusion, the mean SUV_{max} in the tumor group was 1.75 (range: 1.0-9.2) and was significantly higher than that of the nontumor group (mean SUV_{max} 1.1; range: 0.7-2.2; $P < 0.05$). The size and distribution of the pericardial effusions in the tumor group in this study were not significantly different than those in the nontumor group ($P > 0.05$).[43]

The utility of SUV values for distinguishing benign and malignant pericardial disease remains controversial, as these values vary broadly in both settings. Although statistical differences between groups of patients can be demonstrated, the considerable overlap between malignant and nonmalignant cases limits the utility of SUV_{max} values in making this distinction in individual patients, especially when SUV_{max} values are relatively low.

Additional benign causes of pericardial ^{18}F-FDG uptake include fat proliferation of the pericardium,[44] recent cardiac surgery,[45] and a variety of inflammatory and infectious conditions such as constrictive pericarditis, tuberculous pericarditis, and sarcoidosis.[46-51] The etiology of pericardial ^{18}F-FDG uptake may be suggested by the patient's clinical history.

Radiation-Induced Myocarditis

Postradiation myocardial injury occurs as a consequence of microvascular damage, inflammation and, later, fibrosis.[52] During the initial inflammatory stage, myocardial edema is typically localized in a nonvascular distribution. The focal increased ^{18}F-FDG may be misinterpreted as malignant disease. Radiation-induced myocarditis is generally associated with a radiation dose greater than 35 Gy.[53] Unal et al[54] reported annular or focal increased ^{18}F-FDG uptake in the irradiated myocardial segment in patients undergoing radiation for a thoracic malignancy. The authors also reported higher SUV measurements in irradiated

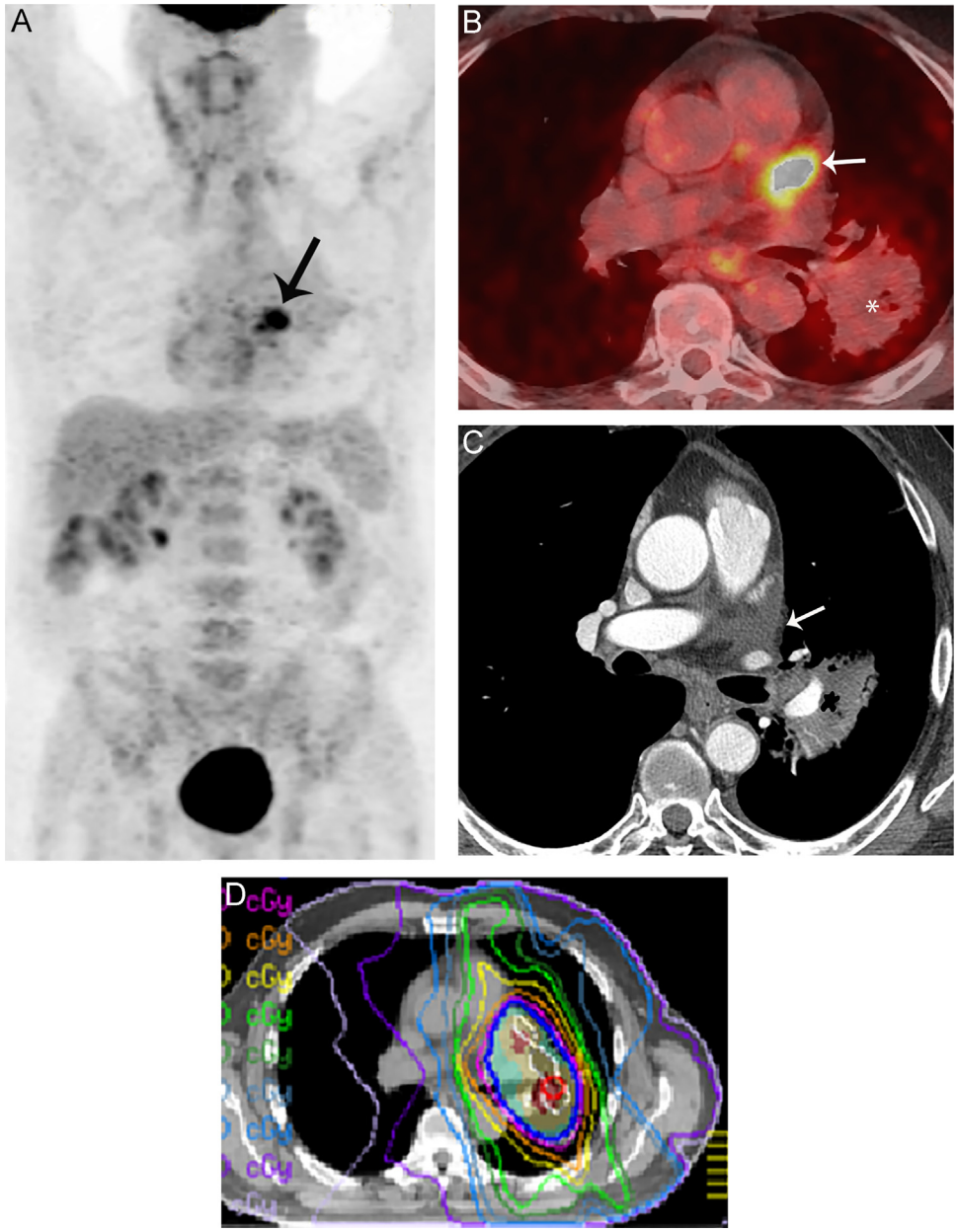

FIG 10. Radiation-induced pericarditis in a man with non–small cell lung carcinoma treated with radiation therapy 6 months before. (A and B) Maximum intensity projection FDG PET (A) and fused axial PET/CT (B) images show increased metabolic activity in the left mediastinum (arrows). The treated malignancy (*) is not FDG avid. (C) Axial contrast-enhanced CT image shows fluid in the transverse (HU 6) pericardial recess corresponding to the increased metabolic activity. (D) Radiation treatment plan confirms inclusion of the transverse pericardial recess within the radiation ports. (Color version of figure is available online.)

segments than in nonirradiated segments in patients with regional myocardial ^{18}F-FDG uptake. Increased ^{18}F-FDG uptake is likely explained by either increased glucose metabolism or decreased fatty acid metabolism in the irradiated myocardium. Localized ^{18}F-FDG activity in the heart of a patient with a history of radiation therapy should be analyzed in light of the radiation port distribution; on occasion, additional dedicated cardiac imaging may be required if the findings are deemed inconclusive on the basis of ^{18}F-FDG PET/CT imaging only.

Idiopathic Hypertrophic Cardiomyopathy

Idiopathic hypertrophic cardiomyopathy (HCM) is a genetic disease characterized by hypertrophic cardiac fibers and is seen in patients of all ages. The affected myocardium in patients with HCM measures more than 1.5 cm in thickness. The clinical course is variable and depends on the location and extent of hypertrophy; the signs and symptoms range from none to angina, syncope and, less frequently, sudden death.[55]

HCM may present as a mass-like lesion involving a segment of the left ventricular wall or septum.[56] In the fasting stage during a routine oncology examination, ^{18}F-FDG uptake by the hypertrophic septal area of the myocardium is usually high and focal, but diffuse ^{18}F-FDG uptake by the left ventricle wall has also been observed.[56] On axial CT images, the mass-like appearance of the myocardium may induce an equivocal diagnosis of myocardial metastasis (Fig 11). Additional cardiac imaging may be necessary to clarify the diagnosis.

Sarcoidosis

Sarcoidosis is a systemic disorder characterized by the presence of noncaseating granulomas. Cardiac involvement is identified

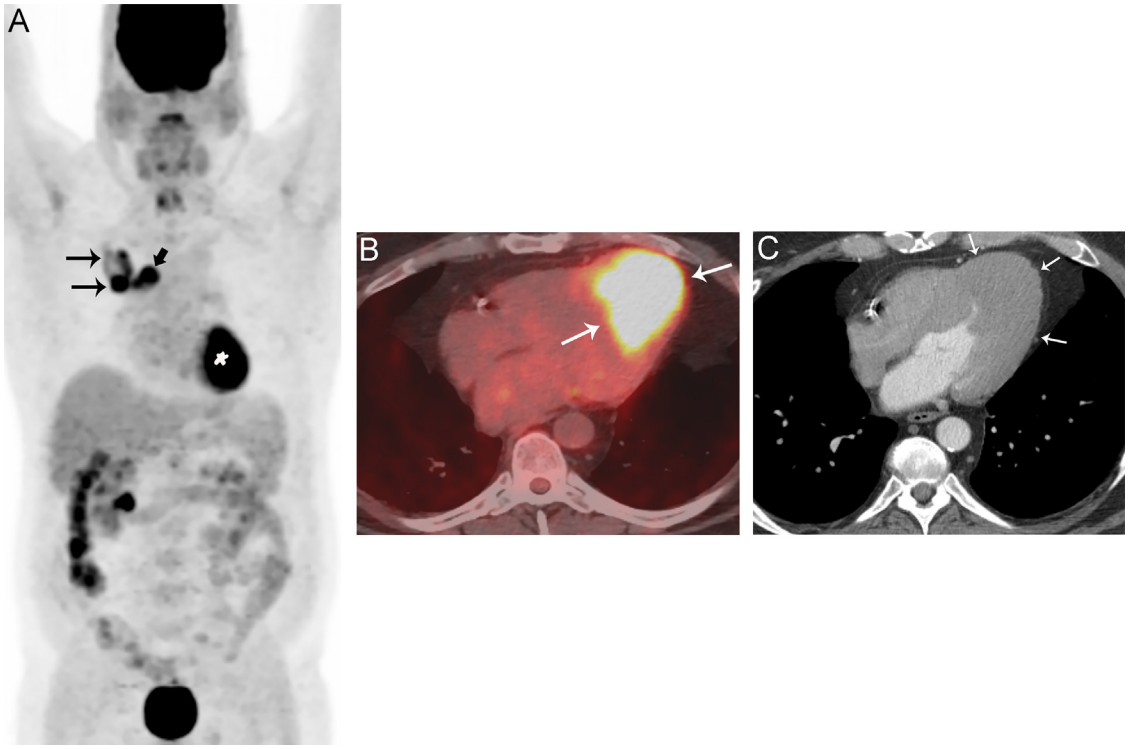

FIG 11. Apical hypertrophic cardiomyopathy in a man with non–small cell lung cancer undergoing disease staging. (A) Maximum intensity projection image shows FDG uptake in the left ventricle (*). The primary malignancy (long arrows) is located in the right upper lobe and there is associated ipsilateral hilar adenopathy (short arrow). (B and C) Fused PET/CT (B) and corresponding axial contrast-enhanced CT (C) images demonstrate increased metabolic activity and thickening (> 1.5 cm) of the apical myocardium (arrows), indicating hypertrophic cardiomyopathy. (Color version of figure is available online.)

clinically in 5% of patients and up to 80% at autopsy.[57,58] Although the prognosis of the disease is poorer with cardiac involvement, cardiac-related symptoms are absent in most patients.[57] ^{18}F-FDG has actually been studied for its utility in the diagnosis and evaluation of therapy response in patients with sarcoidosis.[49,59,60] Dedicated ^{18}F-FDG study for the assessment of myocardial sarcoidosis requires dietary modification with a high-fat, high-protein, and low-carbohydrate diet in order to reduce glucose utilization and ^{18}F-FDG uptake by normal myocardium. In addition to these dietary modifications, extended fasting has been studied showing significant reduction in glucose utilization and ^{18}F-FDG uptake by the myocardium.[61] Extended fasting of greater than 12 hours is currently recommended for myocardial ^{18}F-FDG imaging for sarcoidosis. Some protocols utilize unfractionated intravenous heparin for suppressing myocardial ^{18}F-FDG uptake. intravenous unfractionated heparin activates lipoprotein and hepatic lipases, increasing the

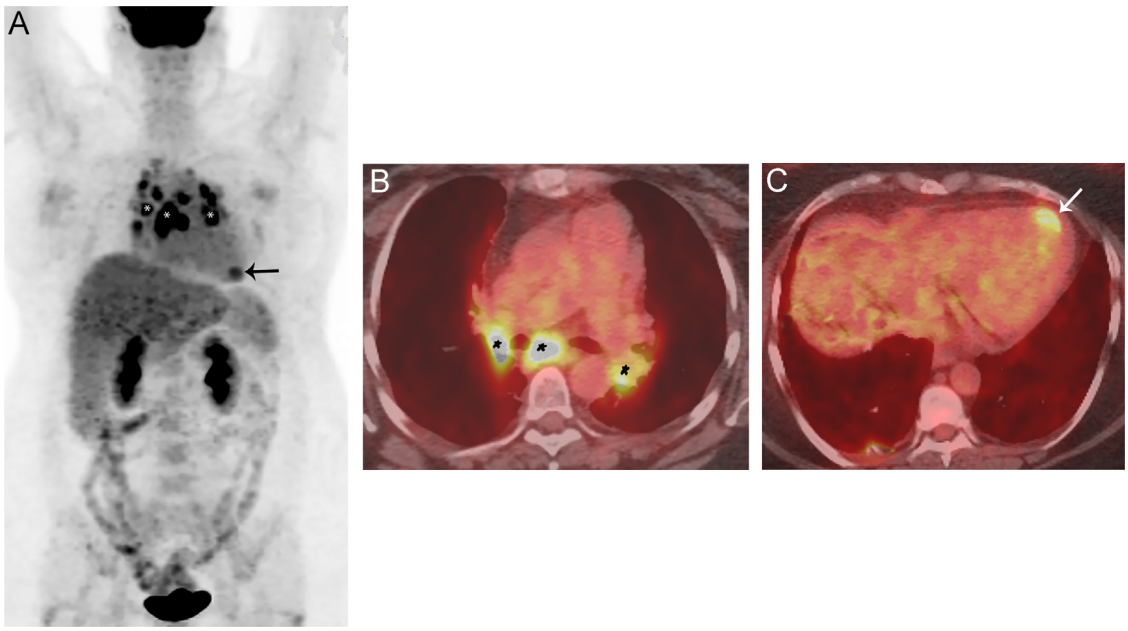

FIG 12. Sarcoid infiltration of the myocardium in a woman in whom lymphoma is suspected. Maximum intensity projection PET (A) and axial fused PET/CT (B and C) images show multicompartmental mediastinal and hilar FDG-avid adenopathy (*) as well as focal FDG uptake in the cardiac apex (arrows), representing myocardial sarcoidosis. (Color version of figure is available online.)

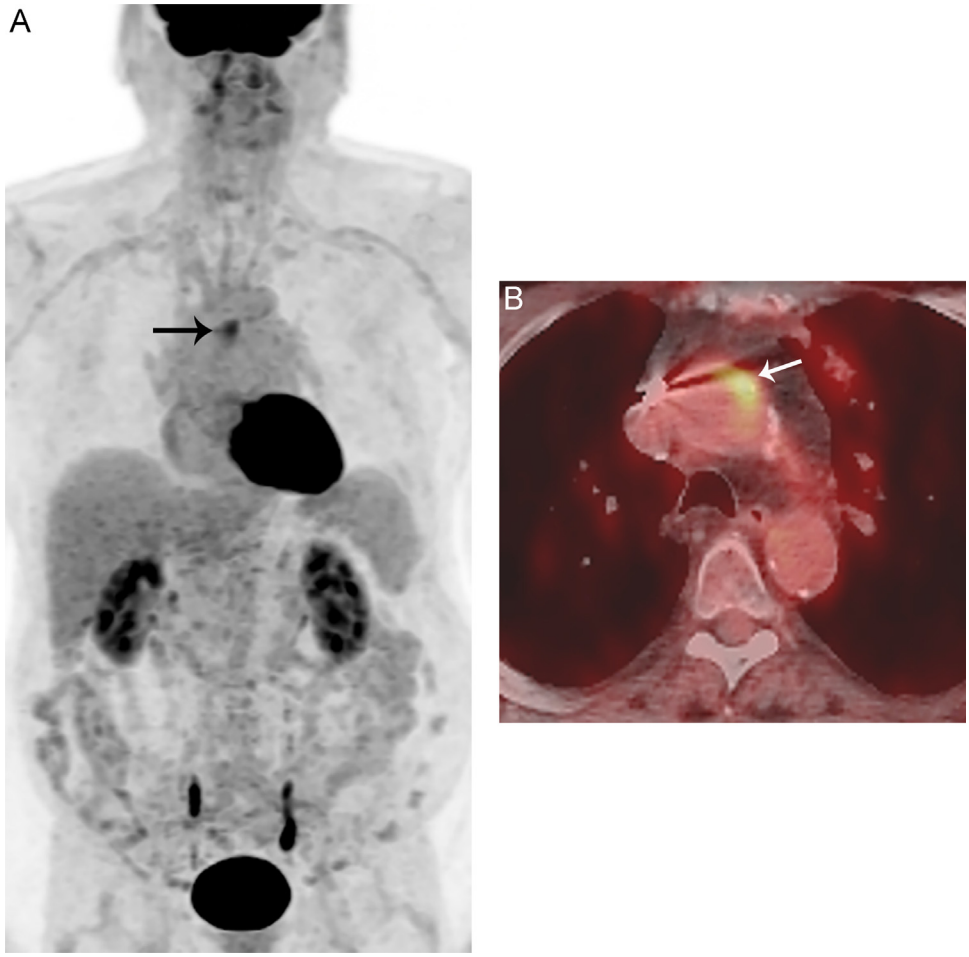

FIG 13. Atheromata of the aortic arch in a man with treated colon cancer. (A and B) Maximum intensity projection FDG PET (A) and fused axial PET/CT images at the level of the aortic arch (B) show focal FDG uptake in the mediastinum localized to atherosclerotic plaque in the aortic arch (arrows), reflecting the active inflammatory nature of the atherosclerotic plaque. (Color version of figure is available online.)

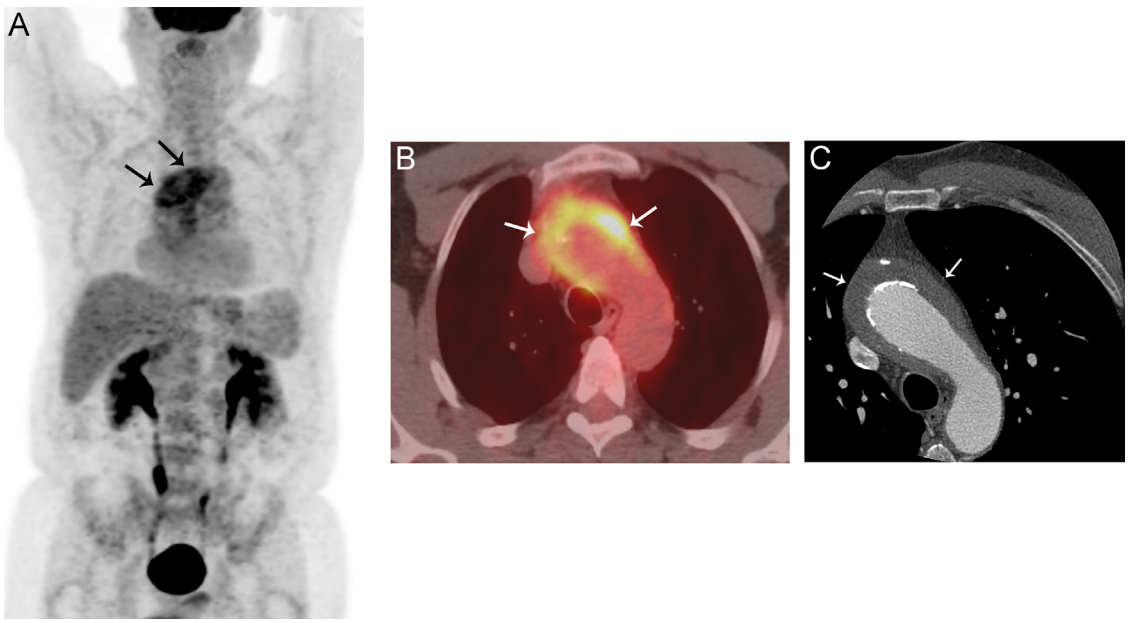

FIG 14. Giant cell arteritis in a patient with treated esophageal carcinoma. Maximum intensity projection FDG PET (A), fused PET/CT (B), and corresponding axial contrast-enhanced CT (C) images show increased metabolic activity and extensive wall thickening at the aortic arch, indicating large-vessel vasculitis. Biopsy of the superficial temporal artery demonstrated giant cell arteritis. (Color version of figure is available online.)

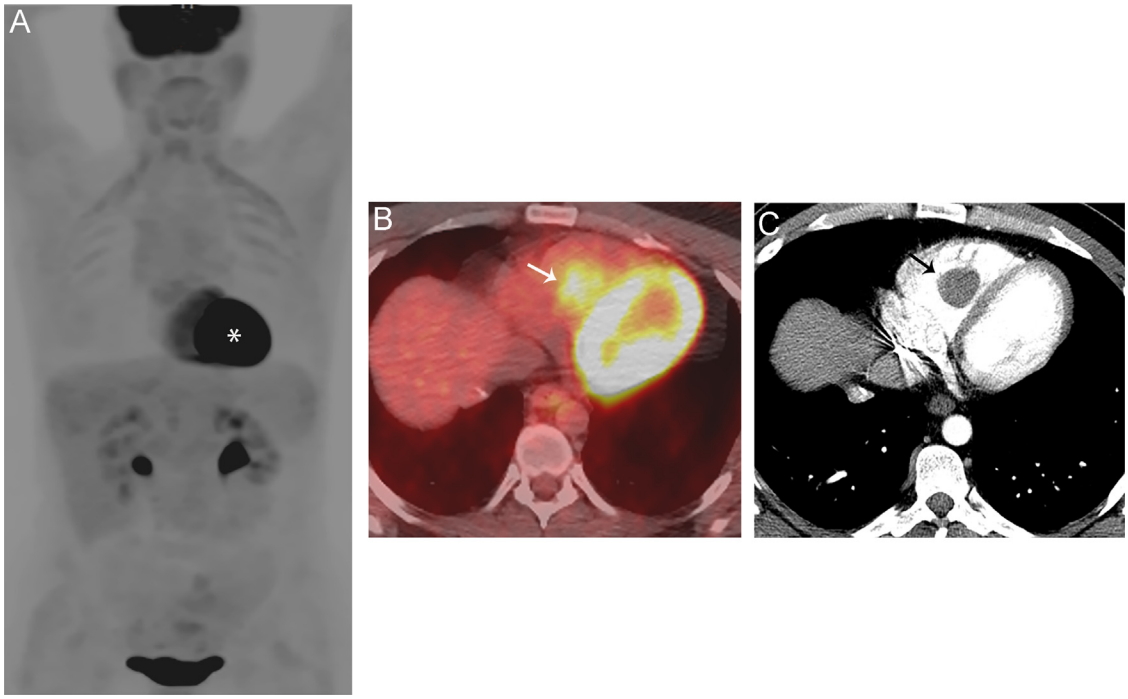

FIG 15. Missed cardiac metastasis in a man with synovial sarcoma. (A) Maximum intensity projection PET image shows normal diffuse FDG uptake in the heart (*). (B) Axial fused PET/CT image shows focal increased FDG uptake in the right ventricle that was considered to be physiological. (C) Axial contrast-enhanced CT image obtained 6 weeks later for evaluation of suspected pulmonary embolism shows a well-defined metastasis in the right ventricle at the site of FDG uptake. (Color version of figure is available online.)

levels of plasmatic free fatty acid levels, and consequently causing a reduction in glucose consumption by normal myocytes.[62]

In oncology patients without known history of sarcoidosis, cases of active inflammation may pose diagnostic challenges, since focal or diffuse myocardial ^{18}F-FDG uptake may be seen and be difficult to distinguish from malignant involvement (Fig 12). The uptake may be explained by accumulation of inflammatory cells with glycolytic activity or by increased myocardial metabolism. A heterogeneous pattern of focal or focal on diffuse uptake is considered characteristic of cardiac involvement by sarcoidosis. Focal intense uptake in the basal septal region is common.[63] In stage I and II sarcoidosis, mediastinal and hilar adenopathy will be present, which may be a clue to the diagnosis. Parenchymal lung disease is seen in 15% of cases, and may increase suspicion for the disease.[64] In PET/CT surveillance studies of patients with known sarcoidosis involving multiple organs, the pattern of multifocal myocardial ^{18}F-FDG uptake may be assumed to be secondary to cardiac sarcoidosis[5] In patients with chronic fibrosing sarcoidosis, no significant metabolic activity is expected.[5]

Atherosclerosis

Atherosclerosis is the result of chronic inflammatory changes to the intimal layer of blood vessels and vascular endothelial cells that results in accumulation of lipids and inflammatory cells within the intima of the vessels. Atherosclerosis affects both large-caliber and small-caliber vessels and can lead to aneurysm formation, obstruction of blood flow by high-grade stenosis, vessel rupture, or distal embolic disease.[23] Most atherosclerotic plaques are not metabolically active on PET/CT imaging.[23] Increased ^{18}F-FDG uptake of arterial walls reflects the inflammatory nature of the disease within active atherosclerotic plaques (Fig 13). Focal or more diffuse accumulation of ^{18}F-FDG can be identified at the aortic wall or following the coronary arteries. Focal ^{18}F-FDG uptake within an atherosclerotic plaque suggests the presence of a marked inflammatory cellular component and increased vulnerability for disruption of it.[65] Isolated ^{18}F-FDG activity within the arterial walls can be confused with mediastinal metastasis. Strict correlation with axial CT and fused PET/CT imaging is essential to confirm vascular disease and distinguish it from metastasis.

Vasculitis (Aortitis)

Inflammatory changes involving the aortic wall occur in large-vessel vasculitis such as Takayasu arteritis and giant cell arteritis (GCA). Takayasu arteritis is a necrotizing, large-vessel panarteritis of unknown cause that is most prevalent in young women ($>$ 80% of cases).[66,67] The disease occurs worldwide but is most prevalent in Asian populations. In contrast, GCA affects people older than 50 years, with a higher prevalence among whites than other racial groups. GCA is the most common form of aortitis in North America, accounting for more than 75% of cases.[68] On PET/CT imaging, the presence of regional, circumferential thickened increased metabolic activity in the aortic wall has been reported as a characteristic finding that is consistent with active disease[23] (Fig 14). On ^{18}F-FDG PET/CT images, ^{18}F-FDG uptake originating within the aortic wall may be difficult to differentiate from activity secondary to metastatic infiltration of the mediastinal fat, especially on noncontrast CT images.

Cardiac and Pericardial Metastases

Cardiac and pericardial metastases are more common than primary cardiac malignancies. The incidence of cardiac metastasis in patients with a known primary tumor is 9%.[69-72] The most common primary tumors that metastasize to the heart are lung cancer, breast cancer, and non-Hodgkin lymphoma.[73] The majority of patients with metastatic disease in the heart and pericardium have no symptoms related to the metastasis.[74] The absence of clinical suspicion and the variable physiological ^{18}F-FDG uptake by the myocardium (even with rigorous fasting) make diagnosis of

cardiac metastasis especially challenging, particularly when the lesion is located in the left ventricle and the "normal" basal-ring pattern obscures the region. Often, the diagnostic clue suggesting malignancy is the presence of similar and persistent focal ^{18}F-FDG uptake in subsequent examinations (Fig 15).

Conclusion

The interpretation of cardiac ^{18}F-FDG uptake in oncology patients is often difficult because of the broad variability of normal physiological metabolic activity. Knowledge of the more common patterns of normal cardiac activity and the patterns resulting from nonneoplastic disease will decrease the likelihood of misinterpretation of PET/CT studies. In addition, correlation with previous imaging studies and clinical and treatment history further facilitates the interpretation of ^{18}F-FDG PET/CT scans, and thus its importance cannot be overemphasized. Careful correlation will preclude additional unnecessary studies or invasive procedures.

References

1. Naveri L, Naveri H, Harkonen M. Myocardial energy metabolism. Ann Chir Gynaecol 1987;76(1):3–11.
2. Shao D, Tian R. Glucose transporters in cardiac metabolism and hypertrophy. Compr Physiol 2015;6(1):331–51.
3. Gropler RJ, Siegel BA, Lee KJ, et al. Nonuniformity in myocardial accumulation of fluorine-18-fluorodeoxyglucose in normal fasted humans. J Nucl Med 1990;31(11):1749–56.
4. Inglese E, Leva L, Matheoud R, et al. Spatial and temporal heterogeneity of regional myocardial uptake in patients without heart disease under fasting conditions on repeated whole-body 18F-FDG PET/CT. J Nucl Med 2007;48(10):1662–1669.
5. Maurer AH, Burshteyn M, Adler LP, et al. How to differentiate benign versus malignant cardiac and paracardiac 18F FDG uptake at oncologic PET/CT. Radiographics 2011;31(5):1287–305.
6. de Groot M, Meeuwis AP, Kok PJ, et al. Influence of blood glucose level, age and fasting period on non-pathological FDG uptake in heart and gut. Eur J Nucl Med Mol Imaging 2005;32(1):98–101.
7. Fukuchi K, Ohta H, Matsumura K, et al. Benign variations and incidental abnormalities of myocardial FDG uptake in the fasting state as encountered during routine oncology positron emission tomography studies. Br J Radiol 2007;80(949):3–11.
8. Lin EC. Isolated papillary muscle uptake on FDG PET/CT. Clin Nucl Med 2007;32(1):76–8.
9. Choi Y, Brunken RC, Hawkins RA, et al. Factors affecting myocardial 2-[F-18] fluoro-2-deoxy-D-glucose uptake in positron emission tomography studies of normal humans. Eur J Nucl Med 1993;20(4):308–18.
10. Tamaki N, Yonekura Y, Kawamoto M, et al. Simple quantification of regional myocardial uptake of fluorine-18-deoxyglucose in the fasting condition. J Nucl Med 1991;32(11):2152–7.
11. Bass A, Stejskalova M, Ostadal B, et al. Differences between atrial and ventricular energy-supplying enzymes in five mammalian species. Physiol Res. 1993;42(1):1–6.
12. Fujii H, Ide M, Yasuda S, et al. Increased FDG uptake in the wall of the right atrium in people who participated in a cancer screening program with whole-body PET. Ann Nucl Med 1999;13(1):55–9.
13. Meka M, Depuey EG, Bhargava P. Focal FDG activity in the region of right atrium: Coregistered CT identifies three benign etiologies. Radiol Case Rep 2008;3(1):120.
14. Kim S, Ding YG, Krynyckyi BR, et al. Increased F-18 FDG uptake in the right auricle of a displaced heart: Potential cause of a false-positive pathologic mediastinal node. Clin Nucl Med 2005;30(2):97–9.
15. Pharr JR, West MB, Kusumoto FM, et al. Prominent crista terminalis appearing as a right atrial mass on transthoracic echocardiogram. J Am Soc Echocardiogr 2002;15(7):753–5.
16. Salustri A, Bakir S, Sana A, et al. Prominent crista terminalis mimicking a right atrial mass: Case report. Cardiovasc Ultrasound. 2010;8:47.
17. Plutchok JJ, Boxt LM, Weinberger J, et al. Differentiation of cardiac tumor from thrombus by combined MRI and F-18 FDG PET imaging. Clin Nucl Med 1998;23(5):324–5.
18. Rinuncini M, Zuin M, Scaranello F, et al. Differentiation of cardiac thrombus from cardiac tumor combining cardiac MRI and 18F-FDG-PET/CT imaging. Int J Cardiol 2016;212:94–6.
19. Turhan S, Ozcan OU, Erol C. Imaging of intracardiac thrombus. Cor et Vasa 2013;55(2):e176–83.
20. Yang T, Wang L, Xiong CM, et al. The ratio of (18)F-FDG activity uptake between the right and left ventricle in patients with pulmonary hypertension correlates with the right ventricular function. Clin Nucl Med 2014;39(5):426–30.
21. Foroulis CN, Kotoulas CS, Kakouros S, et al. Study on the late effect of pneumonectomy on right heart pressures using Doppler echocardiography. Eur J Cardiothorac Surg 2004;26(3):508–14.
22. White CW, Kerber RE, Weiss HR, et al. The effects of atrial fibrillation on atrial pressure-volume and flow relationships. Circ Res 1982;51(2):205–15.
23. James OG, Christensen JD, Wong TZ, et al. Utility of FDG PET/CT in inflammatory cardiovascular disease. Radiographics 2011;31(5):1271–86.
24. Prior JT. Lipomatous hypertrophy of cardiac interatrial septum. A lesion resembling hibernoma, lipoblastomatosis and infiltrating lipoma. Arch Pathol 1964;78:11–5.
25. Reyes CV, Jablokow VR. Lipomatous hypertrophy of the cardiac interatrial septum. A report of 38 cases and review of the literature. Am J Clin Pathol 1979;72(5):785–8.
26. Shirani J, Roberts WC. Clinical, electrocardiographic and morphologic features of massive fatty deposits (lipomatous hypertrophy) in the atrial septum. J Am Coll Cardiol 1993;22(1):226–38.
27. Moinuddeen K, Marica S, Clausi RL, et al. Lipomatous interatrial septal hypertrophy: An unusual cause of intracardiac mass. Eur J Cardiothorac Surg 2002;22(3):468–9.
28. Perez Arroyuelos I, Berastegui Imaz M, Canteli Padilla B, et al. Lipomatous hypertrophy of the interatrial septum associated with fatty replacement of the ventricular myocardium: A case report. J Magn Reson Imaging 2007;26(1):152–4.
29. Page DL. Lipomatous hypertrophy of the cardiac interatrial septum: Its development and probable clinical significance. Hum Pathol 1970;1(1):151–63.
30. Fan CM, Fischman AJ, Kwek BH, et al. Lipomatous hypertrophy of the interatrial septum: Increased uptake on FDG PET. AJR Am J Roentgenol 2005;184(1):339–42.
31. Truong MT, Erasmus JJ, Munden RF, et al. Focal FDG uptake in mediastinal brown fat mimicking malignancy: A potential pitfall resolved on PET/CT. AJR Am J Roentgenol 2004;183(4):1127–32.
32. Pineda V, Caceres J, Andreu J, et al. Epipericardial fat necrosis: Radiologic diagnosis and follow-up. AJR Am J Roentgenol 2005;185(5):1234–6.
33. Webster MW Jr., Bahnson HT. Pericardial fat necrosis. Case report and review. J Thorac Cardiovasc Surg 1974;67(3):430–3.
34. Inoue S, Fujino S, Tezuka N, et al. Encapsulated pericardial fat necrosis treated by video-assisted thoracic surgery: Report of a case. Surg Today 2000;30(8):739–43.
35. Groarke JD, Nguyen PL, Nohria A, et al. Cardiovascular complications of radiation therapy for thoracic malignancies: The role for non-invasive imaging for detection of cardiovascular disease. Eur Heart J 2014;35(10):612–23.
36. Mulrooney DA, Yeazel MW, Kawashima T, et al. Cardiac outcomes in a cohort of adult survivors of childhood and adolescent cancer: Retrospective analysis of the Childhood Cancer Survivor Study cohort. Br Med J 2009;339:b4606.
37. Juweid ME, Stroobants S, Hoekstra OS, et al. Use of positron emission tomography for response assessment of lymphoma: Consensus of the Imaging Subcommittee of International Harmonization Project in Lymphoma. J Clin Oncol 2007;25(5):571–8.
38. Andrade RS, Heron DE, Degirmenci B, et al. Posttreatment assessment of response using FDG-PET/CT for patients treated with definitive radiation therapy for head and neck cancers. Int J Radiat Oncol Biol Phys 2006;65(5):1315–22.
39. Kawabe J, Higashiyama S, Yoshida A, et al. The role of FDG PET-CT in the therapeutic evaluation for HNSCC patients. Jpn J Radiol 2012;30(6):463–70.
40. Boellaard R, Delgado-Bolton R, Oyen WJ, et al. FDG PET/CT: EANM procedure guidelines for tumour imaging: Version 2.0. Eur J Nucl Med Mol Imaging 2015;42(2):328–54.
41. Stewart JR, Fajardo LF. Radiation-induced heart disease: An update. Prog Cardiovasc Dis 1984;27(3):173–94.
42. Shao D, Wang SX, Liang CH, et al. Differentiation of malignant from benign heart and pericardial lesions using positron emission tomography and computed tomography. J Nucl Cardiol 2011;18(4):668–77.
43. Zhang JH, Wang RF, Fan Y, et al. Application of 18F-FDG PET/CT in diagnosis and management of pericardial effusion. J Nucl Med 2014;55:1.
44. Goel SR, Ghesani M, DePuey EG, et al. Abnormal FDG uptake in the Pericardial adipose tissue mimicking malignancy. Radiol Case Rep 2008;3(3):181.
45. Pandit N, Yeung HW. F-18 FDG pericardial uptake secondary to recent cardiac surgery. Clin Nucl Med 2001;26(11):984–5.
46. Chang SA, Choi JY, Kim EK, et al. [18F]Fluorodeoxyglucose PET/CT predicts response to steroid therapy in constrictive pericarditis. J Am Coll Cardiol 2017;69(6):750–2.
47. Dong A, Dong H, Wang Y, et al. 18)F-FDG PET/CT in differentiating acute tuberculous from idiopathic pericarditis: Preliminary study. Clin Nucl Med 2013;38(4):e160–5.
48. Ozmen O, Koksal D, Ozcan A, et al. Decreased metabolic uptake in tuberculous pericarditis indicating response to antituberculosis therapy on FDG PET/CT. Clin Nucl Med 2014;39(10):917–9.
49. Patel D, Xie K, Sweiss NJ, et al. Sarcoid pericarditis and large vessel vasculitis detected on FDG PET/CT. Clin Nucl Med 2016;41(8):661–3.
50. Nunes H, Freynet O, Naggara N, et al. Cardiac sarcoidosis. Semin Respir Crit Care Med 2010;31(4):428–41.
51. Nakao K, Noguchi T, Kim J, et al. Transient constrictive pericarditis diagnosed by cardiac magnetic resonance, 67Ga scintigraphy, and positron emission tomography. Int J Cardiol 2009;137(3):e70–2.
52. Taunk NK, Haffty BG, Kostis JB, et al. Radiation-induced heart disease: Pathologic abnormalities and putative mechanisms. Front Oncol 2015;5:39.
53. Zophel K, Holzel C, Dawel M, et al. PET/CT demonstrates increased myocardial FDG uptake following irradiation therapy. Eur J Nucl Med Mol Imaging 2007;34(8):1322–3.

54. Unal K, Unlu M, Akdemir O, et al. 18F-FDG PET/CT findings of radiotherapy-related myocardial changes in patients with thoracic malignancies. Nucl Med Commun 2013;34(9):855–9.
55. Maron BJ, McKenna WJ, Danielson GK, et al. American College of Cardiology/European Society of Cardiology Clinical Expert Consensus Document on Hypertrophic Cardiomyopathy. A report of the American College of Cardiology Foundation Task Force on Clinical Expert Consensus Documents and the European Society of Cardiology Committee for Practice Guidelines. Eur Heart J 2003;24(21):1965–91.
56. Ishida Y, Nagata S, Uehara T, et al. Clinical analysis of myocardial perfusion and metabolism in patients with hypertrophic cardiomyopathy by single photon emission tomography and positron emission tomography. J Cardiol 2001;37 (Suppl 1):121–8.
57. Silverman KJ, Hutchins GM, Bulkley BH. Cardiac sarcoid: A clinicopathologic study of 84 unselected patients with systemic sarcoidosis. Circulation 1978;58 (6):1204–11.
58. Perry A, Vuitch F. Causes of death in patients with sarcoidosis. A morphologic study of 38 autopsies with clinicopathologic correlations. Arch Pathol Lab Med 1995;119(2):167–72.
59. Okumura W, Iwasaki T, Ueda T, et al. [Usefulness of 18F-FDG PET for diagnosis of cardiac sarcoidosis]. Kaku Igaku 1999;36(4):341–8.
60. Ohira H, Tsujino I, Yoshinaga K. (1)(8)F-Fluoro-2-deoxyglucose positron emission tomography in cardiac sarcoidosis. Eur J Nucl Med Mol Imaging 2011;38 (9):1773–83.
61. Harisankar CN, Mittal BR, Agrawal KL, et al. Utility of high fat and low carbohydrate diet in suppressing myocardial FDG uptake. J Nucl Cardiol 2011;18(5):926–36.
62. Ishimaru S, Tsujino I, Takei T, et al. Focal uptake on 18F-fluoro-2-deoxyglucose positron emission tomography images indicates cardiac involvement of sarcoidosis. Eur Heart J 2005;26(15):1538–43.
63. Yamagishi H, Shirai N, Takagi M, et al. Identification of cardiac sarcoidosis with (13)N-NH(3)/(18)F-FDG PET. J Nucl Med 2003;44(7): 1030–6.
64. Teirstein AS, Machac J, Almeida O, et al. Results of 188 whole-body fluorodeoxyglucose positron emission tomography scans in 137 patients with sarcoidosis. Chest 2007;132(6):1949–53.
65. Wasselius JA, Larsson SA, Jacobsson H. FDG-accumulating atherosclerotic plaques identified with 18F-FDG-PET/CT in 141 patients. Mol Imaging Biol 2009;11(6):455–9.
66. Lupi-Herrera E, Sanchez-Torres G, Marcushamer J, et al. Takayasu's arteritis. Clinical study of 107 cases. Am Heart J 1977;93(1):94–103.
67. Arend WP, Michel BA, Bloch DA, et al. The American College of Rheumatology 1990 criteria for the classification of Takayasu arteritis. Arthritis Rheum 1990;33(8):1129–34.
68. Pacini D, Leone O, Turci S, et al. Incidence, etiology, histologic findings, and course of thoracic inflammatory aortopathies. Ann Thorac Surg 2008;86(5): 1518–23.
69. Bussani R, De-Giorgio F, Abbate A, et al. Cardiac metastases. J Clin Pathol 2007;60(1):27–34.
70. Bruce CJ. Cardiac tumours: Diagnosis and management. Heart 2011;97(2):151–60.
71. Al-Mamgani A, Baartman L, Baaijens M, et al. Cardiac metastases. Int J Clin Oncol 2008;13(4):369–72.
72. Reynen K, Kockeritz U, Strasser RH. Metastases to the heart. Ann Oncol 2004;15 (3):375–81.
73. Lichtenberger JP 3rd, Reynolds DA, Keung J, et al. Metastasis to the heart: A radiologic approach to diagnosis with pathologic correlation. AJR Am J Roentgenol 2016;207:764–72.
74. Butany J, Nair V, Naseemuddin A, et al. Cardiac tumours: Diagnosis and management. Lancet Oncol 2005;6(4):219–28.